

Influence of intrinsic strain on T_c and critical current of high- T_c superconductors

To cite this article: Walter H Fietz *et al* 2005 *Supercond. Sci. Technol.* **18** S332

View the [article online](#) for updates and enhancements.

Related content

- [Phase evolution, structural and superconducting properties of Pb-free \$\text{Bi}_2\text{Sr}_2\text{Ca}_2\text{Cu}_3\text{O}_{10+x}\$ single crystals](#)
B Liang, C Bernhard, Th Wolf *et al.*
- [Anisotropic in-plane reversible strain effect in \$\text{Y}_{0.9}\text{Gd}_{0.1}\text{Ba}_2\text{Cu}_3\text{O}_7\$ coated conductors](#)
D C van der Laan, D Abramov, A A Polyanskii *et al.*
- [Electrical study of an unusual phase transformation in \$\text{aBi}_2\text{Sr}_2\text{Ca}_2\text{Cu}_3\text{O}_{10+x}\$ whisker at room temperature](#)
M Truccato, S Cagliero, A Agostino *et al.*

Recent citations

- [Weak emergence in the angular dependence of the critical current density of the high temperature superconductor coated conductor REBCO](#)
Paul Branch *et al.*
- [Weakly-Emergent Strain-Dependent Properties of High Field Superconductors](#)
Paul Branch *et al.*
- [Biaxial Strain Measurements of JC on a \(RE\)BCO Coated Conductor](#)
Jack R. Greenwood *et al.*



IOP | ebooks™

Bringing together innovative digital publishing with leading authors from the global scientific community.

Start exploring the collection—download the first chapter of every title for free.

Influence of intrinsic strain on T_c and critical current of high- T_c superconductors

Walter H Fietz, Klaus-Peter Weiss and Sonja I Schlachter

Forschungszentrum Karlsruhe, Institut für Technische Physik, Germany

E-mail: walter.fietz@itp.fzk.de

Received 28 July 2005, in final form 4 October 2005

Published 7 November 2005

Online at stacks.iop.org/SUST/18/S332

Abstract

Intrinsic strain is well known to influence T_c and j_c of the classical superconductor Nb_3Sn . Similar effects, which can be even more pronounced, have been found in high- T_c superconductors (HTSs). The HTS properties typically depend on hole doping of the CuO_2 planes. This hole concentration can be influenced by doping with substituting atoms or by changing the oxygen content, which can easily be done for RE- $Ba_2Cu_3O_x$ (RE-123) materials. In addition, the hole doping can be massively influenced by ordering effects within the HTS material and in the case of RE-123 by charge redistribution caused by applied strain and/or pressure. In most cases an anisotropic strain sensitivity is found for HTS materials.

Using literature data from doped RE-123 and new data from uniaxial pressure experiments the possible mechanisms for the change of superconducting properties are analyzed. Finally, literature data from other HTS materials are used to show that similar mechanisms occur for these HTS materials too. Targeting the development of actual HTS conductors these properties may be covered by technical problems yet. However, for future HTS cables the problems arising from uniaxial strain effects have to be addressed.

1. Introduction

For Nb_3Sn it is well known that intrinsic strain is caused by cooling down from reaction temperature, that is necessary to form the superconductor. This strain is increased by the influence of the jacket material, that usually has a higher thermal contraction during cool-down to the operation temperature of 4.5 K. The resulting compressive strain drastically reduces the critical current density j_c .

For HTS material the main challenges are actually to optimize pinning, grain boundaries and grain orientation and to deal with the problem of crack formation and an optimization of the production line for good performance and long lengths with an acceptable price per metre. The R&D work was concentrated on these issues and has led to Bi2223 tapes that can be purchased as an industrial product. For $YBa_2Cu_3O_x$ the problem is to transfer the promising results obtained on short lengths using expensive vacuum methods to cheap non-

vacuum methods that give similar performance for long lengths with an acceptable price per metre. However, when the target has been reached we will have to face similar problems that we know from the well developed Nb_3Sn . We will have to deal with intrinsic strain dependences that for the HTS are not uniform with respect to the strain direction. In addition there are effects that are not known from classical superconductors. We will use $YBa_2Cu_3O_x$ (Y-123) as an example material and demonstrate the different mechanisms influencing the superconducting properties; we will show that most of these are also present for other HTS materials.

From bending experiments it is known that the critical current j_c of thin $YBa_2Cu_3O_x$ films can be massively changed by tension or compression [1]. For tension and higher compression j_c is decreased, which is mainly a consequence of crack formation. However, for small compressions there is a j_c increase and the monitoring of the normal state resistance shows that this is not an effect of crack closure but

should be an intrinsic feature of the material. On the other hand, such a complicated system consisting of a deposited film on a substrate makes it difficult to find the true origin unambiguously. Fortunately, a lot of basic work has been done to investigate the effect of compression on T_c using single crystals or polycrystalline material [2–4].

For HTS materials it has been shown that there is a massive influence of pressure on T_c . The highest T_c reported so far is 164 K at 31 GPa for the Hg1223 compound [5], which demonstrates that hydrostatic pressure can increase the onset of T_c drastically from 135 K at ambient pressure. On the other hand, when other HTS materials are investigated different effects of hydrostatic pressure are found. There is a fast increase with saturation at a moderate pressure of 2 GPa as for Tl2212, a strong negative pressure dependence as for the Tl-221 material or an increase of T_c even to a pressure of 8 GPa as found for $\text{Bi}_{1.68}\text{Pb}_{0.32}\text{Ca}_{1.85}\text{Sr}_{1.75}\text{Cu}_{2.65}\text{O}_x$ [2].

One key to this complex behaviour was to understand the importance of the hole density n_h in the CuO_2 planes which are a common feature of the HTS materials. T_c seems to be determined by the hole density in the CuO_2 planes in a universal way [6, 7], generating a T_c maximum at $n_h = 0.16$ holes/ CuO_2 plane with a parabolic T_c decrease at lower or higher hole densities. Although for different HTS compounds the maximum transition temperature $T_{c,\text{max}}$ at optimal doping $n_{h,\text{opt}}$ is different, a plot of $T_c(n_h)/T_{c,\text{max}}$ as a function of n_h gives one universal parabola. Optical measurements supported the idea of such a parabolic $T_c/T_{c,\text{max}}$ dependence [8] and j_c shows in the slightly overdoped area (beyond the optimum $n_{h,\text{opt}} = 0.16$ holes/ CuO_2 plane) a sharp maximum [9]. To investigate the influence of different hole contents a systematic doping of samples is necessary, which is described in the next section.

A change of the hole content n_h in the HTS material can be initiated by chemical doping or by change of the oxygen content. In the case of RE- $\text{Ba}_2\text{Cu}_3\text{O}_x$ the oxygen content $x = 6 + y$ can be changed very easily because for this material a Cu–O chain layer exists in which the oxygen content y can be varied between $y = 0$ and 1 by annealing the sample at a well defined temperature and oxygen partial pressure [10]. For other materials oxygen can be brought in interstitial sites which, for example, is easy in the case of $\text{Bi}_2\text{Sr}_2\text{CaCu}_2\text{O}_x$ (Bi-2212) but difficult in the case of $(\text{Bi}, \text{Pb})_2\text{Sr}_2\text{Ca}_2\text{Cu}_3\text{O}_x$ (Bi-2223). As a consequence Bi-2122 can easily be optimally doped or even overdoped [11], but for Bi-2223 an annealing under high oxygen pressure of several MPa is necessary to reach optimal doping [12].

In this paper we concentrate on doped RE-123 single crystals to take advantage of the easy adjustability of the hole content n_h by changing the oxygen content with annealing under well controlled conditions as described above. New uniaxial pressure $T_c(p)$ data from an ISTECH $\text{YBa}_2\text{Cu}_3\text{O}_{6.95}$ single crystal are shown. Because of the big crystal size, this crystal [13] allows us to measure uniaxial pressure effects in the a -, b - and c -axis direction directly. The crystal is placed between two sapphire pistons that can be pressed together by means of bellows pressurized with He gas [14]. For T_c determination susceptibility measurements were used. To show the results in a complete picture we first discuss T_c and dT_c/dp of doped RE-123 using published data from

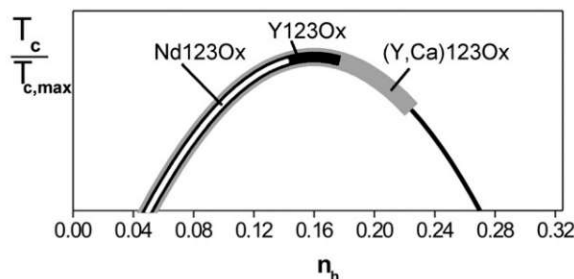


Figure 1. $T_c/T_{c,\text{max}}$ as a function of the hole content n_h of the CuO_2 planes. The Nd-123 samples cover the underdoped region while with the Y-123 samples a slightly overdoped region can be reached. To obtain strongly overdoped samples Ca doping was used.

experiments that have been performed in our group. Starting with hydrostatic pressure experiments on Y-123, Ca doped Y-123 and Nd-123 [4, 15–17] we discuss uniaxial pressure in c -axis direction [4, 17]. This will lead directly to the new measurements of the uniaxial pressure effect in a -, b - and c -axis direction. To complete the picture the effect of oxygen ordering is outlined next, followed by a discussion about if such effects are limited to RE-123 or can be found for other HTS materials too.

2. Effect of hydrostatic pressure on T_c

The universal $T_c/T_{c,\text{max}}(n_h)$ profile of the samples covered by these experiments is shown in figure 1. For Nd-123 the oxygen doping makes the underdoped area accessible. In the case of Y-123 even the slightly overdoped region can be reached. To prepare strongly overdoped samples Y-123 has been doped by substituting 10% or 20% of the Y^{3+} ions by Ca^{2+} ions. The resulting T_c and the pressure effects on T_c , dT_c/dp , of these samples is shown in the left part of figure 2 as a function of the oxygen content x . Obviously it is difficult to make out any kind of systematic context. However, as explained above it is more meaningful to display dT_c/dp as a function of n_h , as was done in figure 2 on the right-hand side. For the overdoped and the weakly underdoped region a linear dependence of $dT_c/dp(n_h)$ is visible. For stronger underdoped samples ($n_h < 0.14$ holes/ CuO_2 plane), dT_c/dp strongly depends on the sample type. This complex behaviour seems to be connected with the occurrence of the ortho-II phase, in which the periodicity of the crystal lattice in the a -axis direction is doubled by the occurrence of alternating full and empty CuO chains and which is most pronounced for Y-123, less visible for Nd-123 and almost suppressed for the Ca-doped samples. The underdoped region will not be discussed in detail in this paper because we will focus on conductors that are relevant for technical applications. More details about the underdoped region can be found in [4]. The $T_c(n_h)$ values plotted in the upper part of the figure have been taken from [8] to demonstrate the cross check of the parabolic $T_c(n_h)$ dependence by determining n_h directly using optical methods. For all samples shown in the present study the n_h values have been calculated using the $T_c(n_h)$ parabola [6, 7]. As a consequence all $T_c(n_h)$ values are exactly on the parabola by definition.

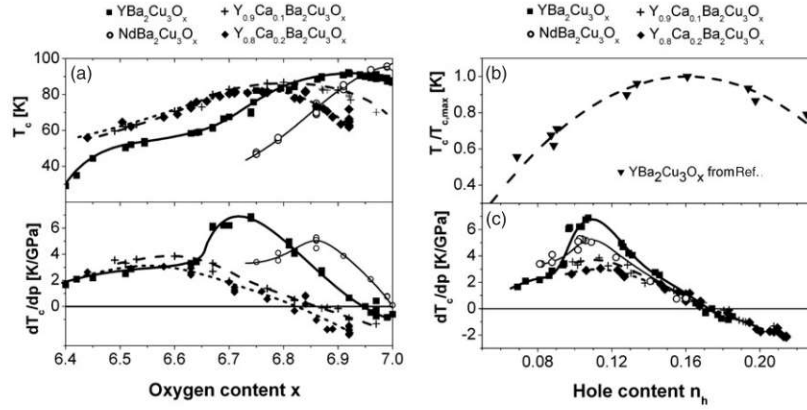


Figure 2. (a) T_c and dT_c/dp of Y123 (■), NdBa₂Cu₃O_x (○), Y_{0.9}Ca_{0.1}Ba₂Cu₃O_x (+) and Y_{0.8}Ca_{0.2}Ba₂Cu₃O_x (◆) as a function of the oxygen content x [4, 15, 17]. (b) $T_c/T_{c,max}(n_h/n_{h,opt})$ from Widder *et al* [8] together with the parabola [6]. (c) dT_c/dp and $\Delta C_p/T_c$ of Y123 (■), Nd123 (○), Y_{0.9}Ca_{0.1}Ba₂Cu₃O_x (+) and Y_{0.8}Ca_{0.2}Ba₂Cu₃O_x (◆) as a function of the hole content n_h per CuO₂ planes [4, 15, 17].

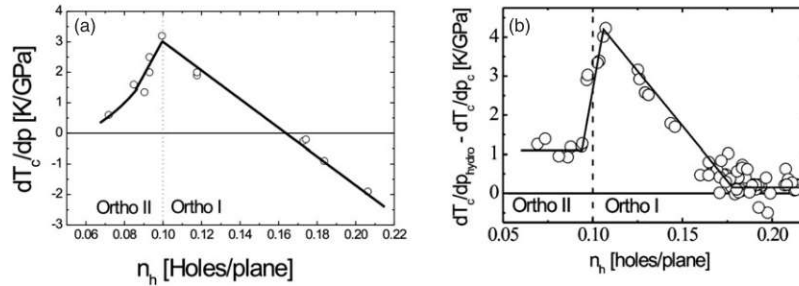


Figure 3. (a) T_c changes due to uniaxial c -axis pressure from several YBa₂Cu₃O_x samples [4, 17]. (b) T_c changes caused by a plane compression $dT_c/dp_{ab} = dT_c/dp - dT_c/dp_c$ of YBa₂Cu₃O_x [17].

3. Effect of uniaxial c -axis pressure

To investigate the origin of the pressure effect dT_c/dp , single crystals have been investigated that allow an oriented application of pressure. For a - or b -axis pressure a uniaxial pressure application is difficult because most single crystals are thin in the c -axis direction and tend to break during pressure application. For c -axis pressure a measurement of dT_c/dp is much easier. Figure 3(a) shows on the left-hand side the dT_c/dp for uniaxial c -axis pressure. The results give for $n_h > 0.1$ holes/CuO₂ plane a linear dT_c/dp dependence with a zero-pressure effect for optimal doped samples at $n_h = 0.16$ holes/CuO₂ plane. This can be explained by assuming a constant hole transfer with the application of c -axis pressure. As a consequence of this simple assumption the pressure effect dT_c/dp is just the derivative of the $T_c(n_h)$ parabola which is shown in figures 1 and 2. This simple picture seems to be valid assuming a hole transfer of 3.1×10^{-3} holes GPa⁻¹ from the overdoped region down to a hole content of 0.11 holes/plane.

It is quite surprising that such a simple model can describe the effect of c -axis pressure. What may be the origin of this hole transfer? A clue to this behaviour has been found in structural investigations under pressure [18]. Neutron investigations showed that the apical oxygen atoms are moved with increasing pressure towards the CuO₂ planes whereas the positive charged Ba atoms move towards the CuO chain

layer (see figure 4). From structural calculations it was found that mainly c -axis pressure is responsible for this movement whereas a - or b -axis pressure do not change the position of these atoms [19]. The shift of the negative charged apical oxygen atoms towards the CuO₂ planes makes it more attractive for holes to go to the CuO₂ planes whereas the shift of the positive charged Ba atom makes it less attractive to be in the CuO chain layer. As a consequence holes are redistributed from the CuO chains to the CuO₂ planes. There is no generation of new holes but this redistribution from the CuO layer to the CuO₂ plane increases the number of holes n_h in the CuO₂ plane.

Knowing the effect of uniaxial c -axis pressure gives the possibility to calculate the effect of a simultaneous compression in a - and b -axis directions which corresponds to a plane compression that may occur when a thin HTS film is deposited on a substrate with a larger thermal contraction during cool-down or even with a lattice mismatch between substrate and superconductor. To calculate this effect of a plane compression for YBa₂Cu₃O_x we use data from hydrostatic experiments [4] and subtract the effect of c -axis compression as displayed in figure 3(a). Figure 3(b) shows the resulting effect of a plane compression. For overdoped and optimal doped samples there is almost no pressure effect visible, whereas dT_c/dp_{ab} increases with decreasing n_h .

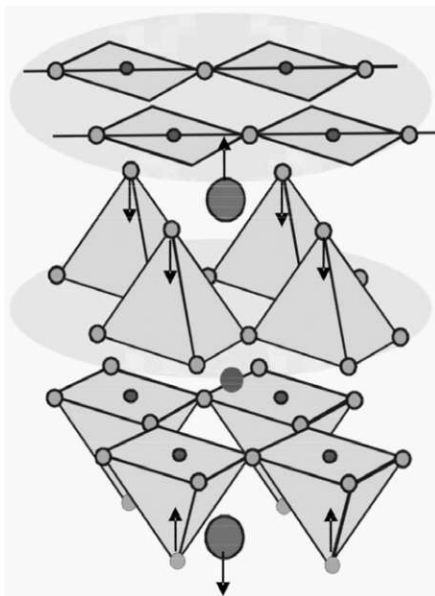


Figure 4. Major changes of atomic positions of $\text{YBa}_2\text{Cu}_3\text{O}_x$ under pressure seen from structural investigations [18] and found by calculating the effect of c -axis pressure [19].

4. Effect of uniaxial pressure in a -, b - and c -axis direction

As the pressure effect of a plane compression for optimal doped $\text{YBa}_2\text{Cu}_3\text{O}_x$ is almost zero, the obvious question is whether the individual pressure effects in a - and b -axis directions give zero-pressure effects, too. As has been argued above, a direct measurement is difficult because such thin crystals tend to break under uniaxial a - or b -axis pressure. However, we had the possibility to measure a thick crystal made by ISTEC [13] with dimensions $a \times b \times c = 1.3 \times 1.5 \times 0.7 \text{ mm}^3$. Figure 5 gives the result of these measurements, which clearly shows that only the pressure effect in the c -axis direction is zero. Applying pressure in the a -axis direction results in a clear decrease of T_c while a compression in the b -axis direction enhances T_c . This shows that the zero pressure effect shown in figure 3 for a plane compression is just a combination of a non-zero a - and b -axis pressure effect which cancel each other. To obtain more information about individual pressure dependences in a -, b - and c -axis direction an indirect method can be used to calculate these values from the jump in the thermal expansion together with T_c , V_{mol} and specific heat data using the Ehrenfest relation (details may be found e.g. in [20]). These investigations confirm the results and show that even for underdoped samples the pressure effects in a - and b -axis directions are non-zero.

The results shown in figure 5 have been obtained by changing pressure at temperatures below 110 K only and the sample was kept during the whole measurement at such low temperatures. That this is essential to obtain correct results will be more clear with the following discussion of oxygen ordering.

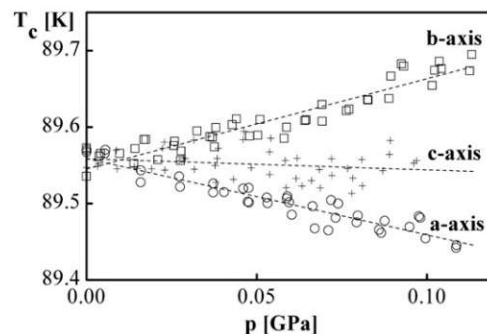


Figure 5. Effect of uniaxial pressure in a -, b - and c -axis directions for $\text{YBa}_2\text{Cu}_3\text{O}_{6.95}$.

5. Effect of oxygen ordering in $\text{YBa}_2\text{Cu}_3\text{O}_x$

The first dT_c/dp measurements reported for $\text{YBa}_2\text{Cu}_3\text{O}_x$ showed a large scatter that was not well understood. The differing results originate in different experimental procedures to measure dT_c/dp and can be seen in figure 6. When pressure is applied at low temperatures (here 85 K, see figure 6(a)) a dT_c/dp of 7.4 K GPa^{-1} is found, but when pressure is changed at 293 K dT_c/dp is increased to 11.5 K GPa^{-1} . The oxygen content was surely not changed because the experiments were performed under helium atmosphere and the full reversibility visible in figure 6 demonstrates that no loss of oxygen occurred (more details can be found in [21, 22]). The origin of these different results can clearly be explained considering systematic quench experiments on oxygen deficient $\text{YBa}_2\text{Cu}_3\text{O}_x$ samples by Claus *et al* [23]. In these experiments samples were quenched from 230 °C and T_c was measured after ageing for different time periods at room temperature. The freshly quenched sample showed no superconductivity, but with increasing annealing time T_c develops, being e.g. 14 K after 14.7 h of annealing or 21 K after 720 h of annealing. A change of the oxygen content at that low temperature could be excluded but this effect could be attributed to oxygen ordering, which forms well defined CuO chains after sufficiently long annealing time at room temperature. After quenching, the oxygen atoms are randomly distributed and there is no hole doping of the CuO_2 planes. Annealing at room temperatures does not change the oxygen content but allows the atoms to move and to form CuO chains. With the formation of these chains during annealing an effective hole doping of the CuO_2 plane begins, which is responsible for the increasing T_c value with increasing oxygen ordering. Using neutron diffraction it was shown that the oxygen ordering process is connected to a shrinkage of the unit cell in the directions of the a -, b - and c -axes [24]. As a consequence, with the application of pressure a higher degree of oxygen ordering is favoured if pressure is applied at temperatures high enough to allow oxygen ordering processes to occur. This is demonstrated in figure 6(b). Directly after pressure application T_c is increased to 70.4 K. Then the sample is brought frequently to room temperature for the time that is displayed in figure 6 (data points 2–8). T_c increases and reaches a saturation temperature of 72 K after approximately 90 h of annealing at room temperature. The same steps are shown in

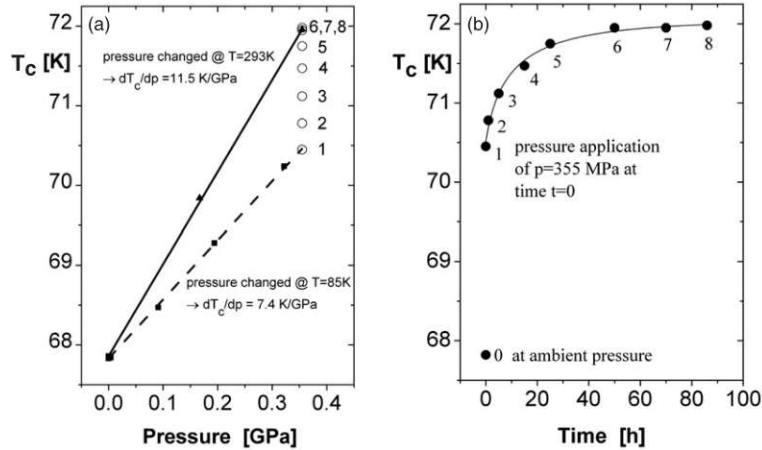


Figure 6. (a) Pressure effect dT_c/dp measured with pressure application at 293 and 85 K including the T_c change with increasing annealing time [21]. (b) T_c increase with time of annealing at 293 K [21].

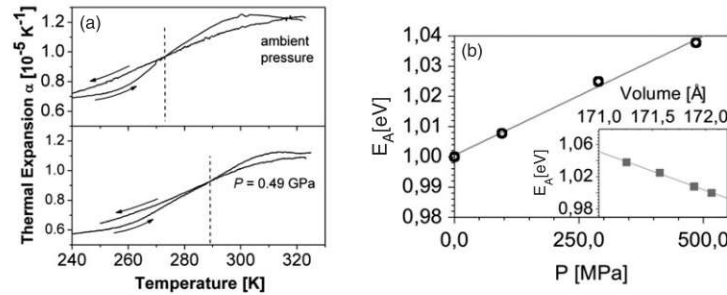


Figure 7. (a) Thermal expansion of $\text{YBa}_2\text{Cu}_3\text{O}_{6.94}$ as a function of temperature. The glassy transition is shifted with the application of pressure [25, 26]. (b) Resulting activation energy E_A of the oxygen ordering process as a function of pressure. As an inset E_A is plotted as a function of the unit cell volume [25, 26].

figure 6(b) and demonstrate that the resulting T_c matches the T_c that is reached with a pressure application at room temperature.

These results clearly show that for $\text{YBa}_2\text{Cu}_3\text{O}_x$ the resulting T_c is not only determined by the oxygen content x , but is massively influenced by oxygen ordering. This oxygen ordering is thermally activated [25, 26] which can be seen in figure 7. The oxygen ordering process is visible in this thermal expansion experiment and upon cooling we find a glassy transition when ordering possibilities are frozen. The ordering temperature is pressure dependent and for an oxygen content of $x = 6.94$ an activation energy of $E_A = 1$ eV is found. Under pressure E_A is increased with $dE_A/dp = 78$ meV GPa^{-1} (see figure 7(b)). As an inset dE_A/dp is shown as a function of the unit cell volume, too.

6. Effect of oxygen ordering and pressure for other HTS materials

At first glance oxygen ordering seems to be restricted to $\text{YBa}_2\text{Cu}_3\text{O}_x$, because only this material has CuO chains where oxygen ordering is well known to occur. On the other hand, investigations of Hg-1201 show that similar effects exist although this compound has no CuO chains [27]. When pressure is applied at room temperature the resulting T_c

changes are clearly different in comparison to experiments where pressure is changed at temperature below 55 K. Similar effects are found for TI superconductors—and again there are no CuO chains [28–30]. For BiSCCO the situation is more complex. Similarly as for other HTS compounds the resulting oxygen content is influenced by the annealing conditions. For the two-layer compound Bi-2212 moderate oxygen partial pressures can be used to obtain an optimally doped sample [11]. Consequently, for higher oxygen partial pressure the T_c is depressed because the sample is overdoped. Ordering effects have not been reported yet, although annealing effects on T_c have been seen for quenched samples recently [31]. For Bi-2223 it is very difficult to obtain optimal samples [12], e.g. a sharp T_c of 109 K is reached by annealing at 500 °C for 100 h and at an oxygen pressure of 10 MPa. When moderate oxygen partial pressures are used the resulting sample will be underdoped and with an increase of the oxygen content the T_c will be higher.

As explained above for RE-123, beside oxygen ordering, pressure can change T_c by pressure induced hole transfer and by a more complex mechanism that results in different signs for a - and b -axis pressure. The pressure induced hole transfer has not clearly been seen for other materials, but different uniaxial pressure dependences even with different signs are very common for HTS materials. For example,

the uniaxial pressure dependences dT_c/dp_i of Bi-2212 are $+1.6 \text{ K GPa}^{-1}$, $+2 \text{ K GPa}^{-1}$ and -2.8 K GPa^{-1} in a -, b - and c -axis directions, respectively [32]. For $\text{La}_{2-x}\text{Sr}_x\text{CuO}_4$ the values are $+7 \text{ K GPa}^{-1}$, $+5.9 \text{ K GPa}^{-1}$ and -13.8 K GPa^{-1} in a -, b - and c -axis directions, but these values change in an individual way with increasing Sr content x [33]. This illustrates that for HTS material, and especially for Bi-compounds and Y-123 that are most interesting for technical applications, we will have a complex strain dependence of superconducting properties. At the moment other problems like phase purity or grain alignment dominate the development of HTS conductors. However, with increasing quality of the production line the described annealing and ordering effects must be considered for the ongoing optimization of these HTS conductors.

7. Conclusion

Different uniaxial pressure dependences dT_c/dp in a -, b - and c -axis directions have been found for $\text{YBa}_2\text{Cu}_3\text{O}_x$, which even show different signs depending on the pressure direction. In the case of optimal and overdoped $\text{YBa}_2\text{Cu}_3\text{O}_x$ the pressure induced charge transfer explains the strong T_c changes by axis compression very well. Additionally, pressure induced ordering effects exist that have their origin in oxygen ordering in the CuO chain layer of $\text{YBa}_2\text{Cu}_3\text{O}_x$. A check of literature data shows that similar effects can be found for other HTS materials, too. For example, LaSCO and BiSCCO show different uniaxial pressure dependences in a -, b - and c -axis directions. Changes of the superconducting properties due to annealing and applied pressure can also be found in Tl and Hg compounds, although no such CuO layers exist. At present for production of HTS tapes of course other problems are dominant, but uniaxial pressure (strain) dependences will surely influence the performance. Charge transfer or ordering effects may be seen for optimized conductors.

References

- [1] Freyhardt H C, Hoffmann J, Wiesmann J, Dzick J, Heinemann K, Issaev A, Usoskin A and Garcia-Moreno F 1996 *Appl. Supercond.* **4** 435–46
- [2] Schilling J S and Klotz S 1992 *Physical Properties of High Temperature Superconductors* vol 3 (Singapore: World Scientific) p 59
- [3] Takahashi H and Mori N 1995 *Studies for High Temperature Superconductors* vol 16 (New York: Nova Science) p 1
- [4] Schlachter S I, Fietz W H, Grube K, Wolf Th, Obst B, Schweiss P and Kläser M 1999 *Physica C* **328** 1–13
- [5] Gao L, Xue Y Y, Chen F, Xiong Q, Meng R L, Ramirez D and Chu C W 1994 *Phys. Rev. B* **50** 4260
- [6] Presland M R, Tallon J L, Buckley R G, Liu R S and Flower N E 1991 *Physica C* **176** 95
- [7] Tallon J L, Bernhard C, Shaked H, Hitterman R L and Jorgensen J D 1995 *Phys. Rev. B* **51** 12911–4
- [8] Widder K, Berner D, Münzel J, Geserich H P, Kläser M, Müller-Vogt G and Wolf Th 1996 *Physica C* **267** 254
- [9] Tallon J L, Williams G V M and Loram J W 2000 *Physica C* **338** 9–17
- [10] Lindemer T B, Hunley J F, Gates J E, Sutton A L Jr, Brynstad J and Hubbard C R 1989 *J. Am. Ceram. Soc.* **72** 1775
- [11] Majewski P 2000 *J. Mater. Res.* **15** 854–70
- [12] Clayton N, Musolino N, Giannini E, Garnier V and Flükiger R 2004 *Supercond. Sci. Technol.* **17** S563–7
- [13] Rykov A I, Jang W J, Unoki H and Tajima S 1996 *Advances in Superconductivity* vol 8, ed H Hayakawa and Y Enomoto (Tokyo: Springer) pp 341–4
- [14] Ludwig H A, Quenzel R, Schlachter S I, Hornung F W, Grube K, Fietz W H and Wolf T 1996 *J. Low Temp. Phys.* **105** 1385
- [15] Schlachter S I, Weiss K P, Fietz W H, Grube K, Leibrock H, Wolf Th, Obst B, Schweiss P, Kläser M and Wühl H 1999 *J. Low Temp. Phys.* **117** 921
- [16] Benischke R, Weber T, Fietz W H, Metzger J, Grube K, Wolf T and Wühl H 1992 *Physica C* **203** 293–8
- [17] Fietz W H *et al* 2000 *Physica C* **341–348** 347–50
- [18] Jorgensen J D, Pei S, Lightfoot P, Hinks D G, Veal B W, Dabrowski D, Pailikas P, Kleb R and Brown I D 1990 *Physica C* **171** 93
- [19] Ludwig H A, Fietz W H and Wühl H 1992 *Physica C* **197** 113
- [20] Meingast C 1996 *J. Low Temp. Phys.* **105** 1391
- [21] Metzger J, Weber T, Fietz W H, Grube K, Ludwig H A, Wolf T and Wühl H 1993 *Physica C* **214** 371
- [22] Fietz W H, Quenzel R, Ludwig H A, Grube K, Schlachter S I, Hornung F W, Wolf T, Erb A, Kläser M and Müller-Vogt M 1996 *Physica C* **270** 258–66
- [23] Claus H, Yang S, Paulikas A P, Downey J W and Veal B W 1990 *Physica C* **171** 205
- [24] Jorgensen J D, Pei S, Lightfoot P, Shi H, Paulikas A P and Veal B W 1990 *Physica C* **167** 571
- [25] Grube K, Leibrock H, Fietz W H, Schlachter S I, Rykov A I, Tajima S, Schweiss P, Obst B and Wühl H 1999 *J. Low Temp. Phys.* **117** 945
- [26] Leibrock H, Grube K, Fietz W H, Schlachter S I, Weiss K P, Rykov A I, Tajima S, Obst B, Schweiss P and Wühl H 2000 *Physica C* **341–348** 439–40
- [27] Sadewasser S, Schilling J S, Wagner J L, Chmaissem O, Jorgensen J D, Hinks D G and Dabrowski B 1999 *Phys. Rev. B* **60** 9827–35
- [28] Sieburger R and Schilling J S 1991 *Physica C* **173** 403
- [29] Klehe A K, Looney C, Schilling J S, Takahashi H, Mori N, Shimakawa Y, Kubo Y, Manako T, Doyle S and Hermann A M 1996 *Physica C* **257** 105
- [30] Takahashi H, Klehe A K, Looney C, Schilling J S, Mori N, Shimakawa Y, Kubo Y and Manako T 1993 *Physica C* **217** 163–9
- [31] Nakao F 2005 *Supercond. Sci. Technol.* **18** S290–6
- [32] Meingast C, Junod A and Walker E 1996 *Physica C* **272** 106–14
- [33] Gugenberger F, Meingast C, Roth G, Grube K, Breit V, Weber T and Wühl H 1994 *Phys. Rev. B* **49** 13137